

## Crossover of the Thermal Escape Problem in Annular Spatially Distributed Systems

Kirill G. Fedorov<sup>1,2</sup> and Andrey L. Pankratov<sup>1,\*</sup>

<sup>1</sup>*Institute for Physics of Microstructures of RAS, GSP-105, Nizhny Novgorod, 603950, Russia*

<sup>2</sup>*Physikalisches Institut, Universität Karlsruhe, Wolfgang-Gaede-Strasse 1, Karlsruhe, D-76131, Germany*

(Received 19 June 2009; published 21 December 2009)

The computer simulations of fluctuational dynamics of an annular system governed by the sine-Gordon model with a white noise source are performed. It is demonstrated that the mean escape time (MET) of a phase string for an annular structure can be much larger than for a linear one and has a strongly pronounced maximum as a function of system's length. The location of the MET maximum roughly equals the size of the kink-antikink pair, which leads to evidence of a spatial crossover between two dynamical regimes: when the phase string escapes over the potential barrier as a whole and when the creation of kink-antikink pairs is the main mechanism of the escape process. For large lengths and in the limit of small noise intensity  $\gamma$ , for both MET and inverse concentration of kinks, we observe the same dependence versus the kink energy  $E_k$ :  $\sim \exp(2E_k/\gamma)$  for the annular structure and  $\sim \exp(E_k/\gamma)$  for the linear one.

DOI: 10.1103/PhysRevLett.103.260601

PACS numbers: 05.40.Ca, 03.75.Lm, 05.45.Yv

The noise-induced dynamics of solitary structures in multistable systems is of great interest in many branches of physics [1]. The sine-Gordon model, often considered in this context, was used for the description of Josephson oscillators and transmission lines [1–8], vortex transistors [9], dislocation theory, and charge density waves in dielectrics, liquid crystals (see [1] for other possible applications), and DNA-promoter dynamics [10]. One of the most important applications of this model is the description of vortex dynamics in the qubits and their readout electronics [5]. To perform the nondestructive readout from qubits, several designs have been suggested, see, e.g., [4,8], which utilize either annular or linear Josephson transmission lines. Because of mathematical difficulties, the temporal characteristics of the noise-induced nucleation of kinks versus the system's length and geometry have not been studied either analytically or numerically. The results of [11–14] are related to the limit of large lengths. Moreover, even in this limit there have been discussions about the temperature dependence of the kink lifetime [12–14]. Therefore, up to now there is no understanding of the optimal length and geometry of spatially extended structures, leading to maximal escape times (i.e., to minimal noise-induced errors).

The quantity of our interest is the mean escape time (MET) of the phase string in a spatially extended structure. The MET is usually the main experimentally relevant characteristic, e.g., in Josephson junctions the MET is the mean time until the generation of noise-induced voltage pulse, which can be measured directly. Our aim is to study the MET of a phase string via computer simulation of the sine-Gordon equation with a white noise. We address the question about the temperature dependence of the MET for different geometries (annular or linear) of the structure and its length. We demonstrate that the fluctuational stability of the annular structure is much higher than for the linear one,

and we specify the optimal length of the former, where the noise-induced errors are minimized.

The sine-Gordon equation for the variable  $\varphi(x, t)$  has the following form (normalized view):

$$\beta \frac{\partial^2 \varphi}{\partial t^2} + \frac{\partial \varphi}{\partial t} - \frac{\partial^2 \varphi}{\partial x^2} = i - \sin(\varphi) + i_f(x, t). \quad (1)$$

The boundary conditions depend on the geometry of the structure, and in the linear overlap case (free boundary case) they have the form:

$$\frac{\partial \varphi(0, t)}{\partial x} = \frac{\partial \varphi(L, t)}{\partial x} = 0, \quad (2)$$

while in the annular case, the periodic boundary conditions have to be used:

$$\varphi(0, t) = \varphi(L, t) + 2\pi n; \quad \frac{\partial \varphi(0, t)}{\partial x} = \frac{\partial \varphi(L, t)}{\partial x}. \quad (3)$$

Here  $\beta = 1/\alpha^2$ ,  $\alpha$  is the damping,  $i$  is the bias force density,  $i_f(x, t)$  is the fluctuational force density, and  $L$  is the dimensionless length of the considered system. In the case where the fluctuations are treated as the white Gaussian noise with zero mean, its correlation function is

$$\langle i_f(x, t) i_f(x', t') \rangle = 2\gamma \delta(x - x') \delta(t - t'), \quad (4)$$

where  $\gamma$  is the dimensionless noise intensity.

Further, we restrict ourselves by considering the overdamped case  $\beta = 0.01$ , similar to Ref. [11–13]. The comparison with the small damping case  $\beta \gg 1$  for the linear structure (1) and (2) has been performed in [15], and the monotonic increase of the MET with the increase of  $\beta$  has been observed; so if  $\beta = 10, 100$ , one will get for  $\tau/\sqrt{\beta}$  roughly the same values as in the presented figures. In terms of Josephson junctions (where the spatial coordinate would be normalized to the Josephson penetration depth), time in Eq. (1) is normalized to the characteristic frequency

[15] rather than to the plasma frequency [6,7], and the noise intensity  $\gamma$  is proportional to the temperature and inversely proportional to the critical current density, while the damping does not enter there [15], satisfying the fluctuation-dissipation theorem [16].

Initially, the phase string  $\varphi(x, 0)$  is located in a potential minimum  $\varphi_0 = \arcsin(i)$  (see Fig. 1, dashed lines), so there are no kinks in the system. Because of the effect of fluctuations, the string  $\varphi(x, t)$  after some time will escape from the initial potential minimum to the next one of the potential  $u(\varphi) = 1 - \cos(\varphi) - i\varphi$  (see Fig. 1, solid curves). At large lengths, it is expected that in the annular structure, due to boundary conditions (3), the escape occurs via the creation of kink-antikink pairs, while in the linear structure in the case (2), the single kinks are created at boundaries [17].

The MET is defined as the mean time of  $\varphi$  residing in the considered interval  $[-\pi, \pi]$  [18,19], where  $P(t)$  is the probability that the phase is located in the initial potential well:

$$\tau = \int_0^{+\infty} t w(t) dt = \int_0^{+\infty} P(t) dt, \quad w(t) = -\frac{\partial P(t)}{\partial t}. \quad (5)$$

Here  $w(t)$  is the probability density of escape time (see [19,20] for details). In difference with the mean first passage time approach, the definition (5) accounts for possible retrapping of the phase string in the initial potential well. The probability  $P(t)$  is computed numerically in the following way: if at the current moment of time  $t > 0$  the realization  $\varphi(x, t)$  is within the interval  $[-\pi, \pi]$ , the probability for the current spatial point of the realization is unity and otherwise zero. The averaging procedure over both  $N$  realizations and over spatial coordinate  $x$  from 0 to  $L$  is performed, and finally the required probability  $P(t)$  is obtained. Numerical solution of the sine-Gordon equation (1) with the boundary conditions (2) and (3) has been computed on the basis of implicit finite-difference scheme [15] with the account of a white noise source. Typical values of discretization steps are  $\Delta x = \Delta t = 0.1-0.02$  and the number of realizations are  $N = 2000-10\,000$ .

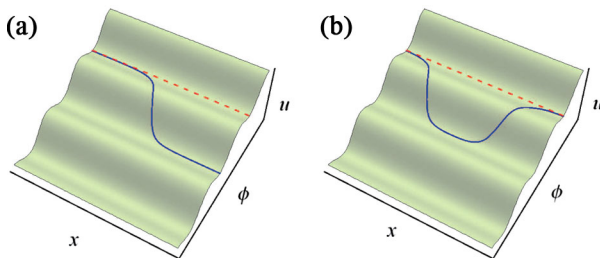


FIG. 1 (color online). Potential profile  $u(\varphi) = 1 - \cos(\varphi) - i\varphi$ ,  $i < 1$ . The dashed line is the initial profile of the phase string. The solid curve is the string in the process of thermally induced escape to the adjacent potential well. (a) Linear structure: one kink is created at the boundary. (b) Annular structure: only kink-antikink pairs can be created due to the absence of boundaries.

Let us plot the MET for the annular structure as a function of length for different values of noise intensity  $\gamma$  and bias force (see Fig. 2). In contrast to the behavior of the MET for the linear geometry with the uniform bias distribution [15] where the MET first increases with the increase of the length and after that remains constant, the MET has a strongly pronounced maximum for the annular case. For the linear structure, the “critical length”  $L \approx 5$ , where the MET reaches the constant, is connected with the possibility for a kink to enter and settle between boundaries. From Fig. 2 one can see that the location of the maximum of the MET for the annular structure is twice larger than the critical length for a linear one. Since boundary conditions (3) admit only the creation of kink-antikink pairs, the size of such a pair fits the location of the maximum rather well. This means that the location of the maximum corresponds to the crossover of two regimes: when the phase string escapes as a whole and when it escapes creating kink-antikink pairs.

It is interesting to plot the MET for different values of bias force ( $i = 0.1, 0.2, 0.36, 0.7$ , and  $0.9$ ) and noise intensity ( $\gamma = 1.55, 1.22, 0.85, 0.3$ , and  $0.077$ ), choosing  $\gamma$  in such a way that the value of  $\tau$  at the maximum is approximately the same (Fig. 3). In this case, the location of the maximum of the MET for the annular structure slightly changes but still remains around  $L \approx 10$ . Considering the tendency of the MET for decreasing  $\gamma$  down to  $0.2$  for the bias force  $i = 0.7$ , we have observed slow migration of the position of the maximum of the MET from  $L \approx 9$  to  $L \approx 11$ . If the bias force is close to the critical value, e.g.,  $i = 0.99$ , and the noise intensity is extremely low,  $\gamma = 0.001$ , we have observed the shift of the maximum of the MET to  $L \approx 15$ , but the qualitative behavior remains the same. The latter case is, however, out of scope of the present Letter and will be studied elsewhere.

The result, indicating the optimal length  $L \approx 10$ , where the maximal noise immunity is reached, is of crucial

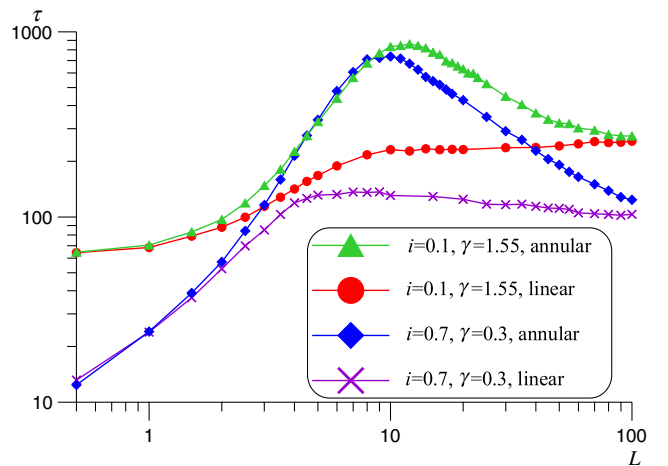


FIG. 2 (color online). The MET for the annular and linear structures.

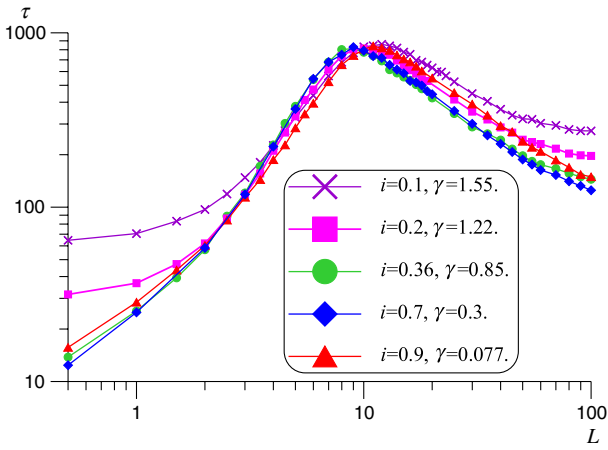


FIG. 3 (color online). The MET for different values of bias current and noise intensity for the annular structure. It is seen that the location of the maximum of the MET remains around  $L \approx 10$ .

importance for creation of fault-tolerant cryoelectronics [4,5] on the basis of long Josephson junctions. While for such devices quantum fluctuations are of importance, due to the general properties of the system, this should affect the actual value of the MET only; however, the location of the maximum should vary weakly. In the following, we choose the length, for which the maximum of the MET is approximately reached, and investigate the dependence of  $\tau$  versus noise intensity  $\gamma$  (temperature dependence, since  $\gamma$  is proportional to the temperature).

As one can see from Fig. 4, in the limit of small noise intensity the factor of the exponent  $\tau \sim \exp(E/\gamma)$ , which fits the computed data, is twice larger for the annular structure ( $E = 2E_k$ ) than for the linear one ( $E = E_k$ ), where  $E_k$  is the kink energy. This confirms that for the annular structure for such a length, the mechanism of creation of kink-antikink pairs predominates, while for

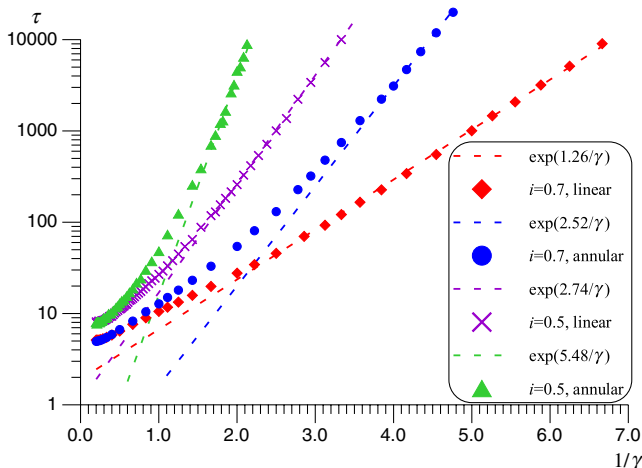


FIG. 4 (color online). Comparison of the temperature dependences of the MET for the annular and linear structures with the length  $L = 10$  and bias  $i = 0.5, 0.7$ .

the linear one, the escape over barrier mostly occurs due to the creation of single kinks at boundaries (see Fig. 1).

The considered range of  $\gamma$  is rather large for practical applications, e.g., for Josephson junctions, where  $\gamma \approx 1$  means that the corresponding thermal current is of the order of critical current. The range of really small  $\gamma$  is not numerically tractable due to exponential dependence of the MET, which leads to exponential increase of the calculation time with the decrease of  $\gamma$ . From the presented plots one can, however, calculate  $\tau(\gamma)$  for any desired values of  $\gamma \ll 1$ , simply extrapolating the straight lines.

For the annular structure of large lengths  $L \geq 10$ , the corresponding numerical factor, the kink energy  $2E_k$ , agrees well with the predictions of Fig. 4 in Ref. [11]. However, for smaller bias  $i = 0.1$  (Fig. 5) the half of the value given by Fig. 4 of Ref. [11] gives good agreement with the MET for linear structure, while for the annular one it slightly overestimates the computer simulation results. For relatively large values of bias starting approximately from  $i \geq 0.5$  and  $L \geq 10$ , the kink energy  $E_k$  agrees well with the formula for the potential barrier height of the potential  $u(\varphi) = 1 - \cos(\varphi) - i\varphi$ , multiplied by a factor of 4:  $E_k = 4\Delta u(i) = 4(2\sqrt{1-i^2} + 2i[\arcsini - \frac{\pi}{2}])$ , which for  $i = 0$  leads to the rest energy of the kink  $E_k = 8$ , as it must [1,11].

From Fig. 2, one may expect that at large lengths the temperature dependence of the annular structure is changed since the MET for linear and annular cases nearly agree. This is, however, true in the large-to-moderate range of noise intensity only. As one can see from Fig. 5, for the lower noise intensities the MET for the annular structure with the length  $L = 100$  perfectly fits the same dependence as for the length  $L = 12$  and with the activation factor of almost twice the activation factor in the linear case. This signals that, namely, the prefactor of the MET is responsible for the maximum of the MET, which in a limit  $\gamma \ll 1$

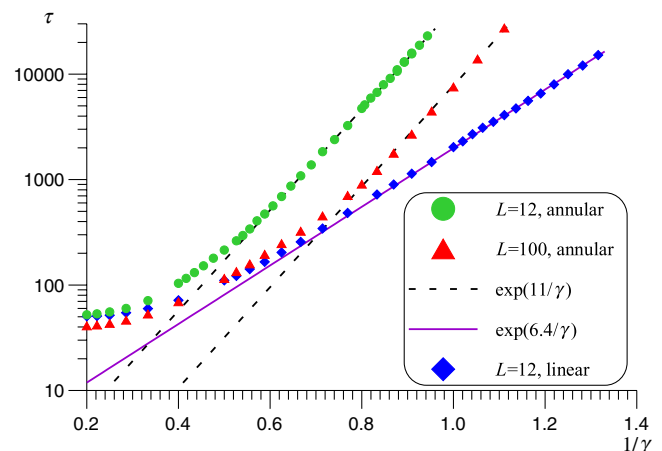


FIG. 5 (color online). Comparison of the temperature dependences of the MET for the annular and linear structures with different lengths and bias  $i = 0.1$ .

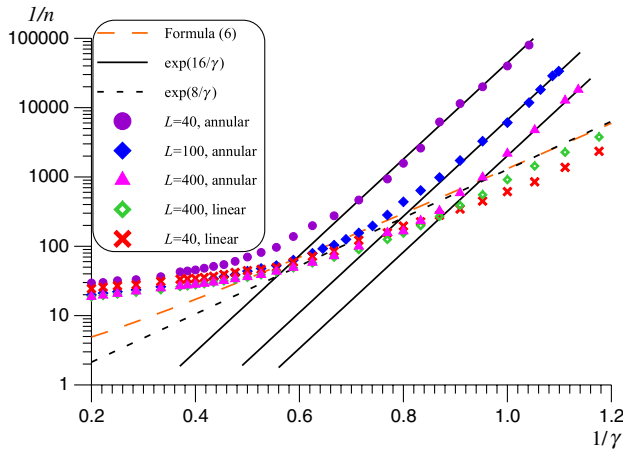


FIG. 6 (color online). Inverse concentration of kinks versus inverse noise intensity in the absence of bias force  $i = 0$ .

gives a difference by roughly a factor of 6 between  $\tau(L = 12)$  and  $\tau(L = 100)$ .

Since we have considered not the kink lifetime [11–13] but the MET, it is wrong to compare our results with the previous predictions directly. However, we have managed to calculate the concentration of kinks  $n$  in the structures for the zero bias force value  $i = 0$ . The results are presented in Fig. 6, where the inverse concentration  $1/n$  is plotted versus the inverse noise intensity.

One can see that for the annular case  $1/n$  perfectly scales as  $\exp(16/\gamma)$ , while in the linear case  $1/n$  is proportional to  $\exp(8/\gamma)$ . Since the rest energy of a kink is equal to 8, see [1,11], this is a clear indication that in the linear structure, the single kinks predominate, while in the annular structure, the kink-antikink pairs are fluctuationally formed. Comparing with the formula for the concentration of kinks from [11,13],

$$n = \sqrt{2E_k/\pi\gamma} \exp(-E_k/\gamma), \quad (6)$$

one can see that the kink concentrations for both linear and annular structures tend to approach the prediction of Eq. (6) with a decrease of  $\gamma$  and an increase of the length, which should be so, since for  $L \rightarrow \infty$  the particular boundary conditions should not be important. Therefore, for both characteristics, the MET and the inverse concentration of kinks, we observe the same dependence versus the kink energy  $E_k$ :  $\sim \exp(2E_k/\gamma)$  for the annular structure and  $\sim \exp(E_k/\gamma)$  for the linear one.

In conclusion, we have demonstrated that fluctuational stability of an annular structure is much higher than for a linear one and specify the optimal length of the former. This optimal length, when the mean escape time reaches the maximum, approximately equals to two critical lengths for the corresponding linear structure, which is also the size of a kink-antikink pair, fluctuationally formed during the escape process. This leads to the evidence of spatial crossover between two dynamical regimes: when the phase string escapes over the potential barrier as a whole and

when the creation of kink-antikink pairs is the main mechanism of the escape process. The obtained results seem to be rather general and should also be observed in other models, such as the  $\phi^4$  model [21], where the same temperature dependence as in [13] was demonstrated. Finally, we note that if there is one kink traveling in an annular structure [4], the optimal length, where the maximal noise immunity will be reached, is obviously around  $L \approx 15\text{--}20$  (the single kink size plus the size of a kink-antikink pair).

The authors wish to thank A. V. Ustinov for useful comments. The work has been supported by RFBR (Projects No. 09-02-00491, No. 09-02-97085, and No. 08-02-97033).

\*alp@ipm.sci-nnov.ru

- [1] Y. S. Kivshar and B. A. Malomed, *Rev. Mod. Phys.* **61**, 763 (1989).
- [2] D. W. McLaughlin and A. C. Scott, *Phys. Rev. A* **18**, 1652 (1978).
- [3] E. Joergensen, V. P. Koshelets, R. Monaco, J. Mygind, M. R. Samuelsen, and M. Salerno, *Phys. Rev. Lett.* **49**, 1093 (1982).
- [4] A. V. Ustinov, *Appl. Phys. Lett.* **80**, 3153 (2002).
- [5] A. Wallraff, A. Kemp, and A. V. Ustinov, in *Quantum Information Processing*, edited by T. Beth and G. Leuchs (Wiley-VCH, Weinheim, 2005), 2nd ed., p. 163.
- [6] A. L. Pankratov, *Phys. Rev. B* **65**, 054504 (2002).
- [7] A. L. Pankratov, *Appl. Phys. Lett.* **92**, 082504 (2008).
- [8] D. R. Gulevich and F. V. Kusmartsev, *Phys. Rev. Lett.* **97**, 017004 (2006).
- [9] K. K. Likharev, V. K. Semenov, O. V. Snigirev, and B. N. Todorov, *IEEE Trans. Magn.* **15**, 420 (1979).
- [10] M. Salerno, *Phys. Rev. A* **44**, 5292 (1991); M. Salerno and Yu. S. Kivshar, *Phys. Lett. A* **193**, 263 (1994); L. V. Yakushevich, A. V. Savin, and L. I. Manevitch, *Phys. Rev. E* **66**, 016614 (2002); A. Kundu, *Phys. Rev. Lett.* **99**, 154101 (2007).
- [11] M. Buttiker and R. Landauer, *Phys. Rev. A* **23**, 1397 (1981).
- [12] P. Hanggi, F. Marchesoni, and P. Sodano, *Phys. Rev. Lett.* **60**, 2563 (1988).
- [13] M. Buttiker and T. Christen, *Phys. Rev. Lett.* **75**, 1895 (1995).
- [14] P. Hanggi and F. Marchesoni, *Phys. Rev. Lett.* **77**, 787 (1996); M. Buttiker and T. Christen, *ibid.* **77**, 788 (1996).
- [15] K. G. Fedorov and A. L. Pankratov, *Phys. Rev. B* **76**, 024504 (2007).
- [16] M. Salerno, E. Joergensen, and M. R. Samuelsen, *Phys. Rev. B* **30**, 2635 (1984); M. Salerno, M. R. Samuelsen, and H. Svensmark, *Phys. Rev. B* **38**, 593 (1988).
- [17] T. Christen, *Europhys. Lett.* **31**, 181 (1995).
- [18] A. N. Malakhov and A. L. Pankratov, *Physica (Amsterdam)* **269C**, 46 (1996).
- [19] A. N. Malakhov and A. L. Pankratov, *Adv. Chem. Phys.* **121**, 357 (2002).
- [20] A. L. Pankratov, *Phys. Lett. A* **234**, 329 (1997).
- [21] S. Habib and G. Lythe, *Phys. Rev. Lett.* **84**, 1070 (2000).